

# Sustainable Water Responsive Mechanically Adaptive and Self-Healable Polymer Composites Derived from Biomass

## Authors:

Pranabesh Sahu, Anil K. Bhowmick

Date Submitted: 2020-09-23

Keywords: self-healing, mechanically adaptive behavior, water-sensitivity, cellulose nanofibrils, poly (myrcene-co-furfuryl methacrylate), green composites

## Abstract:

New synthetic biobased mechanically adaptive composites, responding to water and having self-healing property, were developed. These composites were prepared by introducing plant-based cellulose nanofibrils (CNFs) at 10, 20, and 25% (v/v) concentration into a biobased rubbery poly (myrcene-co-furfuryl methacrylate) (PMF) matrix by solution mixing and subsequent compression molding technique. The reinforcement of CNFs led to an increase in the tensile storage modulus ( $E'$ ) of the dry composites. Upon exposure to water, water sensitivity and a drastic fall in storage moduli ( $E'$ ) were observed for the 25% (v/v) CNF composite. A modulus reduction from 1.27 (dry state) to 0.15 MPa (wet state) was observed for this composite. The water-sensitive nature of the composites was also confirmed from the force modulation study in atomic force microscopy (AFM), revealing the average modulus as 82.7 and 32.3 MPa for dry and swollen composites, respectively. Interestingly, the composites also showed thermoreversibility and excellent healing property via Diels-Alder (DA) click chemistry using bismaleimide as a crosslinker, when the scratched samples were heated at 120 °C (rDA) for 10 h and then cooled down to 60 °C (DA) followed by room temperature. The healing efficiency was obtained as about 90% from the AFM 3D height images. Thus, the composites exhibited dual stimuli-responsive behavior as mechanically adaptive water sensitive polymers with water as the stimulus and self-healing polymer using bismaleimide as an external stimulus. Therefore, this study provides guidance and new frontiers to make use of composite materials based on biopolymers for various potential smart and biomedical applications.

Record Type: Published Article

Submitted To: LAPSE (Living Archive for Process Systems Engineering)

Citation (overall record, always the latest version):

LAPSE:2020.1001

Citation (this specific file, latest version):

LAPSE:2020.1001-1

Citation (this specific file, this version):

LAPSE:2020.1001-1v1

DOI of Published Version: <https://doi.org/10.3390/pr8060726>

License: Creative Commons Attribution 4.0 International (CC BY 4.0)

Article

# Sustainable Water Responsive Mechanically Adaptive and Self-Healable Polymer Composites Derived from Biomass

Pranabesh Sahu <sup>1,\*</sup>  and Anil K. Bhowmick <sup>1,2,\*</sup> <sup>1</sup> Rubber Technology Centre, Indian Institute of Technology Kharagpur, Kharagpur 721302, West Bengal, India<sup>2</sup> Department of Chemical and Biomolecular Engineering, The University of Houston, 4726 Calhoun Rd, Houston, TX 77204-4004, USA

\* Correspondence: pranabesh.cema@gmail.com (P.S.); akbhowmick@uh.edu or anilbhowmick@gmail.com (A.K.B.)

Received: 10 May 2020; Accepted: 19 June 2020; Published: 22 June 2020



**Abstract:** New synthetic biobased mechanically adaptive composites, responding to water and having self-healing property, were developed. These composites were prepared by introducing plant-based cellulose nanofibrils (CNFs) at 10, 20, and 25% (*v/v*) concentration into a biobased rubbery poly (myrcene-*co*-furfuryl methacrylate) (PMF) matrix by solution mixing and subsequent compression molding technique. The reinforcement of CNFs led to an increase in the tensile storage modulus ( $E'$ ) of the dry composites. Upon exposure to water, water sensitivity and a drastic fall in storage moduli ( $E'$ ) were observed for the 25% (*v/v*) CNF composite. A modulus reduction from 1.27 (dry state) to 0.15 MPa (wet state) was observed for this composite. The water-sensitive nature of the composites was also confirmed from the force modulation study in atomic force microscopy (AFM), revealing the average modulus as 82.7 and 32.3 MPa for dry and swollen composites, respectively. Interestingly, the composites also showed thermoreversibility and excellent healing property via Diels-Alder (DA) click chemistry using bismaleimide as a crosslinker, when the scratched samples were heated at 120 °C (rDA) for 10 h and then cooled down to 60 °C (DA) followed by room temperature. The healing efficiency was obtained as about 90% from the AFM 3D height images. Thus, the composites exhibited dual stimuli-responsive behavior as mechanically adaptive water sensitive polymers with water as the stimulus and self-healing polymer using bismaleimide as an external stimulus. Therefore, this study provides guidance and new frontiers to make use of composite materials based on biopolymers for various potential smart and biomedical applications.

**Keywords:** green composites; poly (myrcene-*co*-furfuryl methacrylate); cellulose nanofibrils; water-sensitivity; mechanically adaptive behavior; self-healing

## 1. Introduction

'Sustainable', 'sustainability' and 'sustainable development' are the theme of today's scientific world which is guiding the progress of the next generation of materials and products [1,2]. The majority of the polymers used in modern life are derived from petrochemicals. The vast increase in the production and application of synthetic polymers has also created negative impacts on several environmental issues, such as the depletion of fossil resources, global warming and climate change. Owing to these severe environmental concerns related to the use of synthetic polymers, society is being encouraged to adopt green consumerism as a primary approach to curb these problems [3,4]. Considering this issue, the ongoing progress in biobased polymers toward general and engineering applications is the only possible alternative [5–7]. The utilization of biobased polymers is supported by recent government incentives, e.g., the United States Department of Agriculture (USDA) BioPreferred Program [8].

This program, and others like it, has helped to increase consumer awareness and greater demand for biobased products. Nowadays, biobased polymers are being applied to general and engineering applications in many areas like packaging, composites, coatings, fibers or material reinforcement, as well as for smart applications such as self-healing and stimuli-responsive materials [9–12].

The current growth of polymer biocomposites is of notable interest to academic researchers and industrial organizations [13]. These materials show useful properties by combining fillers and a polymer matrix and cover a wide range of properties that are useful for multiple applications, such as sporting goods, automobile parts, and aerospace components [14]. In the coming years, there will be an increasing tendency to develop green composite materials from plant resources to provide ecofriendly, high-performance biobased products [15,16]. Green composites are materials which have environment-friendly attributes that are technically and economically feasible while reducing the level of pollution.

The blooming of synthetic adaptive polymer composites which are sensitive to water has gained considerable attention from research professionals in scientific and technological areas [12,17]. This type of stimuli-responsive mechanically adaptive composite is considered to be a biomimetic and promising material for biomedical applications [17,18]. Stimuli-responsive polymers or composites change their properties upon exposure to external stimuli, for example heat, light, water, chemicals, magnetic fields, etc. Polymer nanocomposites with cellulose nanofibrils/whiskers are major examples of water-responsive mechanically adaptive materials [19]. Biobased polymer composites using plant-derived micro- and nano-size cellulosic fibers are appealing to replace man-made fibers as reinforcement fillers to produce eco-efficient products for high performance and smart applications. Cellulose nanofibrils (CNFs) are biobased, biodegradable, and can be derived from several renewable sources, including wood pulp, cotton and tunicates [20]. Polymer composites were prepared by using various processes, such as solution casting, compression molding, and emulsion polymerization by introducing biobased cellulose nanofibrils or nanofibers into a rubbery polymer including polybutadiene [21], styrene-butadiene rubber (SBR) [22], and polyurethane rubbers [23]. These composites reported earlier show mechanically adaptive behavior with response to water, mimicking the behavior of sea cucumbers present in the sea [24]. Although the uses of cellulose nanofibers were biobased, the polymer matrix used for the preparation of the above composites was entirely petroleum-based synthetic elastomers [21–23]. There have been attempts to make use of bio-derived polymers as the matrix to prepare high-value water-responsive composites [25]. There have been no studies on polymyrcene or polyfurfural or their copolymer-based composites so far. Also, multifunctional composites, for example with water sensitivity along with a self-healing nature, are important to develop for future applications.

Motivated by the desire to develop smart and stimuli-responsive composites with mechanically adaptive nature, we have integrated cellulose nanofibrils (CNFs) into a rubbery polymer synthesized from renewable resources. Thereby, this study provides the thrust within the scientific community to make use of biobased polymers for the production and development of synthetic stimuli-responsive composites. The preparation of water-responsive elastomer CNFs composites was carried out by utilizing biobased synthesized polymer, poly (myrcene-*co*-furfuryl methacrylate) (PMF) [26] as the matrix via solution casting approach. Poly (MY<sub>80</sub>FMA<sub>20</sub>) (PMF-20) polymer was chosen for composite preparation due to its partially polar nature, good rubbery property and good compatibility with the CNFs' hydrophilic sites. The preparation, properties, aqueous swelling behavior and dispersion of CNF composites were explored in this research. Water sensitivity of the composites with respect to the storage modulus ( $E'$ ) was also investigated. The initial stiffness was followed when the composite was dried. Force modulation microscopy (FMM) via AFM imaging was also used to detect variations in the mechanical properties such as modulus and adhesion of the dry and swell sample surface. In addition, self-healing characteristics of the composites (PMF/CNFs) using bismaleimide (BM) as an external cross-linker following Diels-Alder (DA) click chemistry have been studied. The thermoreversible behavior of the polymer network (PMF-20/CNF/BM) was analyzed by DSC analysis. The self-healing

phenomenon and recovery of the crosslinked polymers films was verified by optical microscopy and atomic force microscopy (AFM). Thus, the prepared polymer composite was used to study two different stimuli-responsive phenomena; one is the water-sensitive composite using water as an external stimulus, and the other is the self-healing nature of the composite using bismaleimide as an external crosslinker. Both the above properties have been investigated using the same PMF/CNFs composite. Keeping in mind the immense advantages of sustainable polymers, this study primarily focuses on the performance as well as basic and smart applications of cellulose nanofibrils based green composites from renewable resources.

## 2. Experimental

### 2.1. Materials

Poly (myrcene-*co*-furfuryl methacrylate) (PMF) polymer with 80/20 comonomer composition of myrcene (MY) and furfuryl methacrylate (FMA) was synthesized according to the earlier reported procedure [26] and selected for the preparation of biobased composite. The detailed synthetic procedure is also specified later. Poly (MY<sub>80</sub>FMA<sub>20</sub>), number-average molecular weight,  $M_n = 59,900$  Da, polydispersity index, PDI = 1.6 was chosen as the polymer matrix for the fabrication of green composite. Cellulose nanofibrils (CNFs) in the form of granules (Curran<sup>®</sup>, Density = 1.07g/cm<sup>3</sup>) were supplied by CelluComp Limited, Scotland, UK. Anhydrous tetrahydrofuran (THF) was purchased from E. Merck Ltd., Mumbai, India. 1,1'-(Methylenedi-4,1-phenylene) bismaleimide as a crosslinker was procured from Sigma-Aldrich, Bengaluru, India for the self-healing study. The solvents used were of analytical grade quality and purified prior to use. Deionized water (DI H<sub>2</sub>O) was used for all the experiments.

### 2.2. Fabrication of Biobased Poly (MY-*co*-FMA) (PMF) Polymers

PMF elastomer was synthesized using the redox emulsion polymerization technique following the recipe reported earlier [26]. Copolymer with 80/20 comonomer composition of MY and FMA was synthesized at room temperature (RT) for 20 h reaction time. In a round-bottom flask, at first, distilled water, potassium oleate, potassium chloride, and potassium phosphate buffer were added and stirred for 15–20 min at 300 rpm. After the time, both the monomers were charged by micropipette into the reaction mixture and were mixed for further 30 min to obtain a stable emulsion. Thereafter, the redox couple solution was injected into the reactor and the reactor was maintained at an inert atmosphere by flushing with nitrogen gas. Then, the initiator was added into the flask. The polymerization reaction was carried at 25 °C for 20 h. After the end of the reaction, the milky latex was coagulated using excess ethanol to obtain the polymer. The precipitated rubbery polymer was cleaned with deionized water many times and vacuum dried in an oven for 24 h at 50 °C. The yield of the copolymers obtained was about 56%. At higher temperatures, the polymerization formed a highly crosslinked product because of the existence of furan moiety in FMA. So, the reaction condition for polymerization was optimized and set at lower temperature, i.e., RT. Figure 1 shows the schematic view of the polymerization reaction. The detailed kinetics and characterization of polymer were reported by us previously [26].

### 2.3. Preparation of PMF/CNFs Composite Films via Solution Casting Approach

The polymer poly (MY<sub>80</sub>FMA<sub>20</sub>) was dissolved in THF at a concentration of 20 mg/mL by stirring for 4–5 h. Cellulose nanofibrils (CNFs) of same concentration was dispersed in THF by stirring for 1 day and ultra-sonicated using an Elma Transsonic TI-H5 sonicator, Germany for 2–3 h at room temperature. Curran<sup>®</sup> Granules was added at the dispersion phase for the formulation of nanocomposites. Composites comprising of 10, 20 and 25% (*v/v* unless otherwise noted) CNFs were fabricated by combining the requisite amount of the cellulose nanofibrils dispersion and the polymer solution, stirring for 4–5 h and ultra-sonicating for 1 h. The resulting homogeneous mixture was casted onto Teflon petridishes. The solvent was vaporized at 60 °C for 48 h and thereafter vacuum

dried at 50 °C for 24 h to remove any excess solvent. The schematic diagram for the preparation of biobased composites is shown in Figure 2. Using latex of the polymer and cellulose nanofibrils, similar composite films were also made. As we had studied water sensitivity, the THF cast samples were used for this investigation to avoid the effect of residual water and the water cast samples were discarded. Poly (MY<sub>80</sub>FMA<sub>20</sub>) (PMF-20) polymer was chosen for composite preparation due to its partial polar nature, good rubbery property and compatibility with the CNF hydrophilic filler.

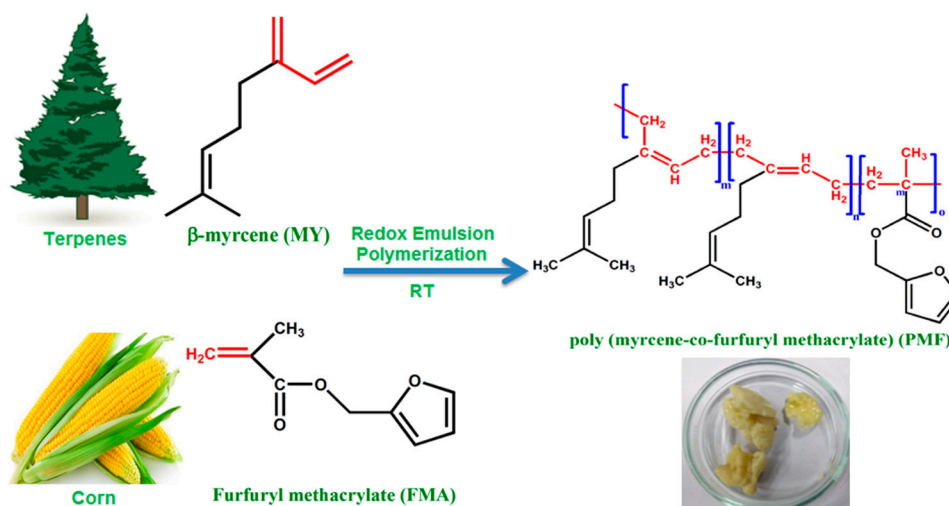


**Figure 1.** Synthetic routes toward  $\beta$ -myrcene/furfuryl methacrylate copolymers (Reproduced with permission from Wiley, Sahu, P.; Bhowmick, A.K., *J. Polym. Sci. Part A Polym. Chem.*, published by Wiley, 2019).

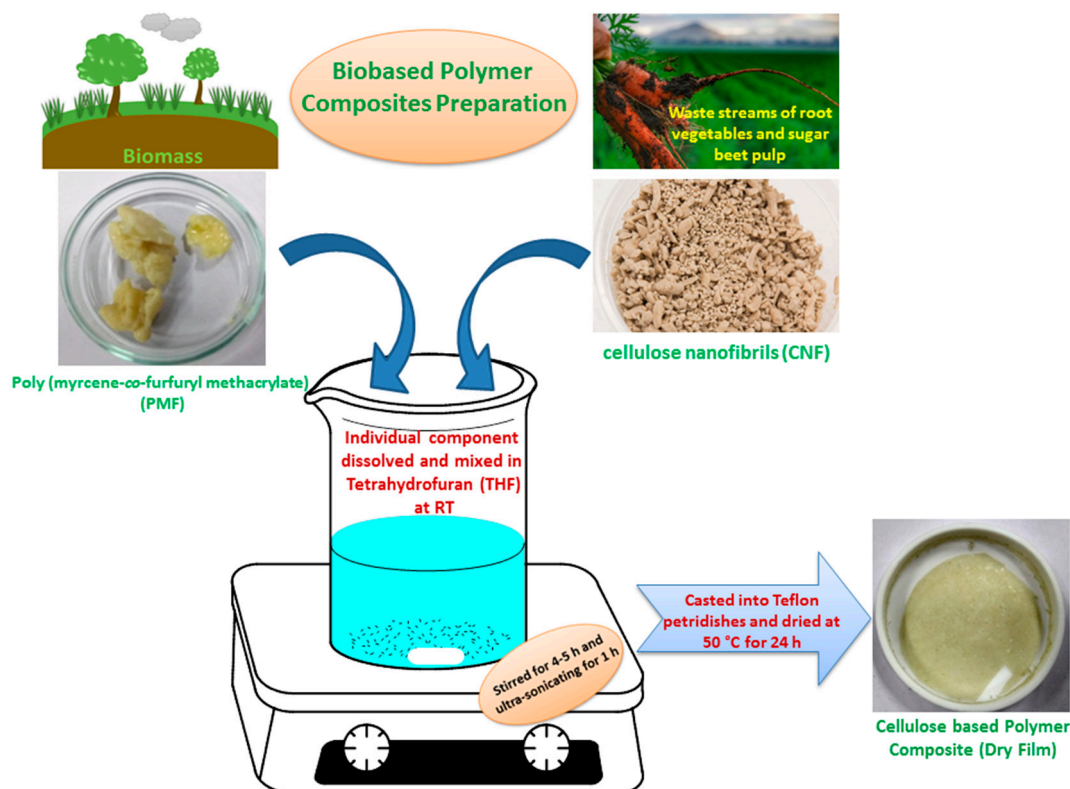


**Figure 2.** Schematic diagram for the preparation of biobased poly (myrcene-co-furfuryl methacrylate)/cellulose nanofibrils (PMF/CNFs) composites.



The dried films were subsequently compression molded in a Moore Press (George E. Moore & Sons Ltd., Birmingham, UK) at 60 °C and 1000 psi for 2.5 min to yield a 100–200 µm thick nanocomposite films. Initial sample with lower CNFs content showed extensive shrinking after pressing at room temperature, which decreased substantially with the increasing volume fraction of CNFs. Higher temperature pressing was also used to reduce the shrinkage problem, but such conditions only resulted to yellowing of the films and degradation of the polymer. The pressing condition was optimized to obtain non-shrinking films. The shrinking behavior of the material with lower loading i.e., 10% CNFs was quantified. Initially, the pressing temperature was increased from room to a higher temperature (60 °C) to obtain free-standing films. However, at a lower temperature, there was an extensive shrinkage mainly due to the sticky low-molecular weight pristine PMF polymer. With increase in temperature, the problem was solved with the CNFs content (variation) due to the greater stiffness of the composites.

#### 2.4. Preparation of PMF/CNFs and Bismaleimide Films for Self-Healing Analysis via DA Reaction

PMF/CNFs composite and bismaleimide (BM) (1:1 molar ratio) were treated separately in tetrahydrofuran solvent in glass vials. BM was used as a crosslinker for the study of DA reaction. The solutions were mixed and the reaction mixture was heated to 60 °C and kept for stirring for 10–12 h under nitrogen atmosphere. The liquid solution transformed into viscous gel after stirring, resulting in the formation of crosslinked solid polymeric adduct. The resulting PMF/BM crosslinked adduct was insoluble in organic solvents such as tetrahydrofuran, toluene, and dimethyl sulfoxide at room temperature. However, the polymer in the crosslinked adduct was soluble upon heating at 120 °C for 8–10 h, indicating the disconnection of the furfuryl ring present in the polymer and BM via retro-DA reaction. The DA-crosslinked formation and characterization study was followed according to our previous published study [26].

#### 2.5. Characterization

The morphological behavior of the composites and CNFs were observed via both atomic force microscopy and scanning electron microscopy analysis. Park Systems NX10 instrument (Suwon, Korea) under tapping mode was used for AFM analysis. The rate of scanning and employed lift height were set at 1.0 Hz and 11.2 µm (varied when required), respectively, for observing the dispersion of CNFs in the composites. To examine the morphology of the composites, thin films were mounted on a clean glass microscopy slides and samples were scanned following the above conditions. ZEISS field emission scanning electron microscopy (FESEM), Carl ZEISS SMT, Germany was also used to overview the distribution of the cellulose nanofibrils in the composites. Thin dry films were used, and the surface morphology was observed. The dispersion was observed by soaking the nanocomposites in a mixed solution of THF and chloroform (1:1) to partially dissolve the elastomer part (PMF) and uncover the CNFs before SEM analysis. Gold coating was done on the sample surface before the experiment and an acceleration voltage of 5 kV was applied for analysis. The morphology of CNFs was also characterized individually.

The swelling degree was calculated by immersing the pristine and the composite films in deionized water at RT. A rectangular specimen of specific thickness, 5 mm width and 20 mm length, was cut for the swelling experiment and the test was done over a period of 5 days. The sample was removed every 24 h, soaked in a filter paper, weighed and again sunk in deionized water. The degree of swelling was calculated using the standard procedure [25,27], given by Equation (1):

$$\text{Swelling degree (\%)} = \frac{W_t - W_o}{W_o} \times 100 \quad (1)$$

where  $W_t$  and  $W_o$  are the mass of the wet and dry sample respectively.

The Fourier-transform infrared spectroscopy (FTIR) of the composites (dry and swollen samples) was taken in the range of 400–4000  $\text{cm}^{-1}$  on a PerkinElmer Spectrum 400 spectrometer (Waltham, MA, USA). This was to investigate the effect of swelling on the furan group present in the composite.

## 2.6. Water Sensitive Behavior of the Biobased Composites

The water-responsive mechanical behavior of the polymer composite was characterized using a dynamic mechanical thermal analyzer, METRAVIB 50N (Chemin des Ormeaux, Limonest, France), operating in tension mode. Temperature sweep measurements in the range of 15–30 °C were followed at a frequency of 1.0 Hz and 0.1% dynamic strain at a ramp rate of 3 °C/min for both the dry and the wet films. Each dry and wet sample was dried under vacuum prior to DMA testing. In order to establish the mechanical behavior of the composite films in the wet state, the samples were immersed in deionized water at RT for 4 to 6 days and then wiped with filter paper to remove residual water for the analysis. In order to determine the kinetics of softening and stiffening of the wet sample, a controlled experimental condition (within the rubbery region @ 25 °C) was followed i.e., from 15 to 30 °C. The change in the storage modulus of the dry and wet sample over the temperature range was compared for the water responsive behavior.

Force modulation imaging in contact mode using AFM (Park Systems NX10, Suwon, Korea) was carried out to detect sample stiffness as well as the mechanical properties of the composite (PMF-20/CNF) in dry and swollen states. The AFM tip was scanned in contact with the sample surface (four different regions selected). The scan rate and amplitude were maintained at 0.6 Hz and 25.0 µm respectively. From the force modulation image, using the Hertzian contact mechanics model, the quantitative average value of the Young's modulus of sample surface was taken into consideration (dry and swollen states). The local adhesion force between the tip and the surface under inspection was also obtained from the imaging.

## 2.7. Self-Healing Behaviour of the Biobased Composites

The self-healing character of the composites was monitored by optical microscopy (Leica DM LM, Ernst-Leitz-Strasse, Wetzlar, Germany). The cross-linked polymer mixture was placed on a glass slide and dried for microscopic analysis. The composite films were then notched with a knife and the healing was performed by heating the cut samples at 120–130 °C for 10 h along with subsequent cooling to 60–70 °C for few hours and then to ambient temperature. The healing was confirmed from the optical microscopy images of notched crosslinked polymer composite films (before and after healing). Only dry composites were used for the healing study. The reasons for this are described later by FTIR analysis.

Thermo-reversibility of the prepared DA-network (PMF-20/CNF/BM) was characterized by a NETZSCH DSC 200F3Maia (Selb, Germany) differential scanning calorimeter (DSC). The samples were heated from –100 to +200 °C at a heating rate of 10 °C/min under N<sub>2</sub> atmosphere. The  $T_g$  value of pristine PMF-20 was obtained from the second heating run of the experiment. The coupling (DA) and decoupling (rDA) nature of the thermoreversible network was verified from the first heating and the cooling scans of DSC.

The self-healing nature of the biocomposites was observed in Park Systems NX10 AFM instrument (Suwon, Korea) under tapping mode. A thin crosslinked film of biobased composite was prepared and a gentle scratch was made with a razor blade. Initially, a cut of 2 µm average depth was made on the film and scanned for imaging. The set point and scan rate were set at 11.2 µm and 0.6 Hz, respectively. The healing was observed by heating the cut sample at 120–130 °C for 10 h followed by cooling down to room temperature. The healing efficiency was calculated from the height image calculation of the sample (before and after healing).

The self-healing character of the PMF/CNF/BM composite was our prime focus following DA-click chemistry using bismaleimide as the external stimulus. Although the degree of swelling was investigated in water for the PMF/CNF/BM composite, due to the presence of crosslinking between the bismaleimide and furan in PMF, the swelling percentage was observed as much less (7–8% in 5 days) for the composite. Therefore, only uncross-linked composites (without bismaleimide) were used for the water-responsive investigation study.

### 3. Results and Discussion

#### 3.1. Morphology of CNFs and Dispersion of CNFs in the Composites

Figure 3a,b shows the AFM and SEM images of the CNFs, which indicate that before processing into composites, the CNFs are well separated and display a network of isolated nanofibrils and some globular shape fibril aggregates. The average diameter of the fibers was found to be in the range of 10–40 nm from the SEM image. AFM and SEM photographs on larger area show that the fibers are slightly agglomerated.

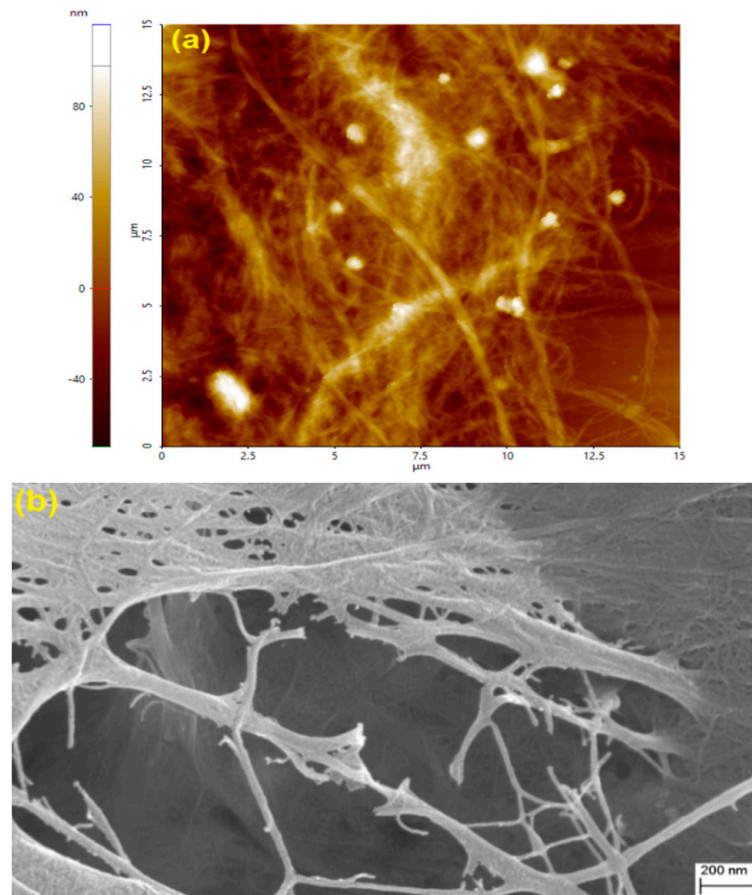


**Figure 3.** (a) Atomic force micrograph (height image) and (b) Scanning electron microscope image of pure CNFs.

The dispersion of CNFs in the composite was also observed from the AFM and SEM micrographs. The composites with 10 and 25% (*v/v*) concentration of CNFs are shown in Figure 4a–d. From the images, it is obvious that CNFs are distributed uniformly and surrounded by the elastomer matrix. This is due to the hydrogen bonding between the ester or furan groups of the PMF-20 elastomer matrix and the surface hydroxyl groups of CNFs. Good dispersion of CNFs also suggests a stronger interaction between the filler and the matrix. Fibrils in the form of nanorods are embedded deeply into the polymer matrix (as shown by the arrows in Figure 4c,d). The distribution is uniform, even with higher fibril content, i.e., 25% (*v/v*) of CNFs in the SEM image.



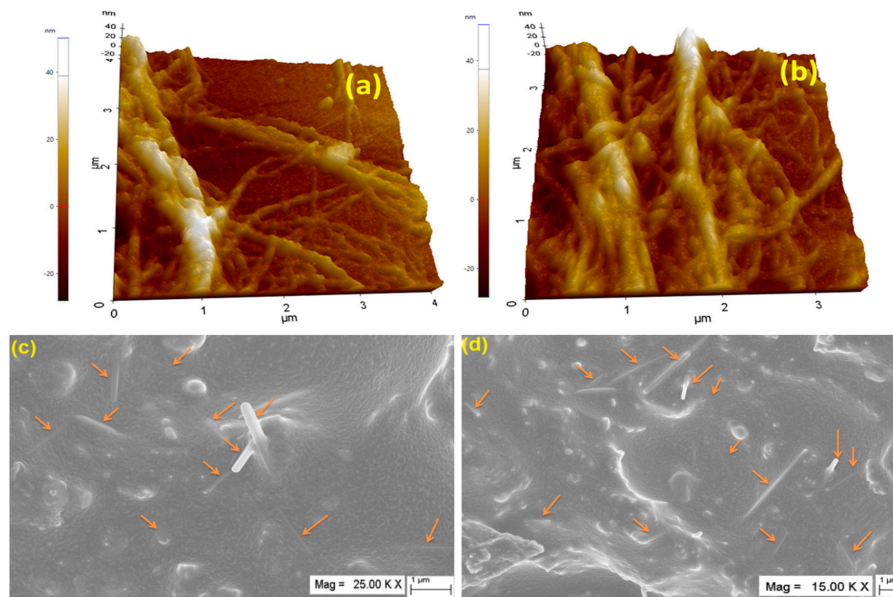


**Figure 4.** (a,b) AFM images of PMF-20/CNF composite with 10 and 25% (*v/v*) CNFs; (c,d) SEM images of PMF-20/CNF composite with 10 and 25% (*v/v*) CNFs.

AFM images (Figure 4a,b) show slight agglomeration in contrast to nanofibrils, as seen in the SEM image. The aggregation of nanofibrils forms the filler–filler interaction or network. At higher CNF content, the filler–filler network formation predominates, and the composite lacks uniform dispersion of CNFs. At lower CNF content, CNFs are distributed uniformly in the polymer matrix without much agglomeration.

### 3.2. Aqueous Swelling Behavior of PMF/CNFs Composites

The capability of water uptake of the PMF/CNF composites was investigated in deionized water to determine the influence of swelling on the mechanical properties. Pristine polymer (PMF-20) showed less swelling compared to the composites subjected to water. The swelling percentage was still in the range of 20–22%, which may be due to the presence of cross-linkable polar furan group. Compression molded films with nanofibril contents of 10, 20 and 25% (*v/v*) were subjected to swelling for 5 days at room temperature. The degree of swelling increases gradually with time, as is the typical nature of diffusion phenomena, and also increases with the nanofibril content in the composite, as shown in Figure 5. These are typical curves for the diffusion of permeant through a film. In general, with increasing filler content, the swelling increases (hydrophilic nature of CNFs). At a particular time, swelling degree was higher with higher fiber loading. The mechanical integrity of the composites depends on how CNFs interact with the polymer as well as the composition.

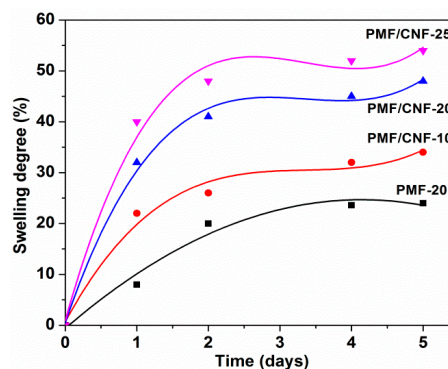


**Figure 5.** Swelling of PMF-20 and PMF/CNF composite films in deionized water as a function of CNFs amount and immersion time.

This phenomenon can be ascribed to the increased hydrophilicity of the composite because of the existence of cellulose fibrils, which promotes the diffusion of water through the polymer matrix. In common, the water uptake rate reaches an equilibrium value roughly after 2 days of swelling. The swelling phenomenon of PMF/CNF composites with 25% CNFs after 2 and 5 days is pictorially presented in Figure 6.

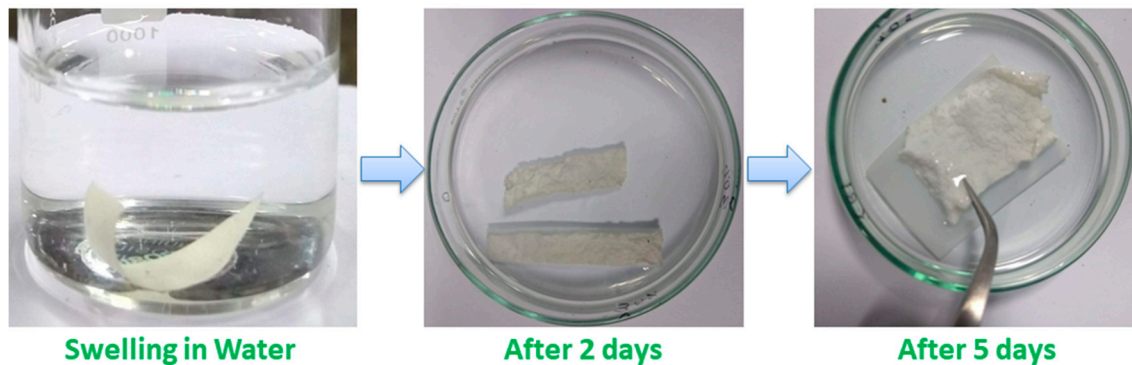


**Figure 6.** Swelling of composite films with 25% CNFs in deionized water with time.

### 3.3. Mechanical Properties and Water Responsive Behavior of PMF/CNFs Composites

The thermo-mechanical properties of these composites were investigated using dynamic mechanical analysis. Figure 7 shows the storage modulus ( $E'$ ) as a function of composition and temperature for all the composites. Table 1 summarizes the value of  $E'$  in the rubbery region (25 °C) for the dry and water-swollen composites. In all three series of polymer/CNF composites,  $E'$  increases steadily with the CNFs concentration, due to greater reinforcement in the polymer matrix. Interfacial interactions (hydrogen bonding) between the PMF polymer and CNFs contribute to the increase in the storage modulus. The wet stage tensile storage modulus ( $E'$ ) of the composites was measured after swelling in deionized water for 4 and 6 days at room temperature. Interestingly, all the water swollen samples showed a significant reduction in  $E'$  compared to the dry samples. The largest contrast was noticed for the sample having 25% ( $v/v$ ) CNF, due to substantial water absorption. A modulus reduction from 1.27 (dry state) to 0.15 MPa (wet state) was observed for the composite containing 25% CNFs. In the other two cases, the contrast was smaller still, but  $E'$  showed a decrease for the water swollen samples. This confirms that the water-sensitive nature of the green composites depends on the content of CNFs. The decrease in the modulus can be attributed to how the water diffuses into the film and reduces the stiffness. Up to a certain concentration, the water diffuses through the polymer network formed between the polymer and the fibers. After that, the extent of swelling is mainly governed by the residual nanofibers, i.e., in the case of 25% CNF composite. Therefore, the modulus drop was observed more for PMF/CNF-25 where the hydrophilic nature of CNFs mainly assists the swelling phenomenon. However, in the case of PMF/CNF-20 and PMF/CNF-10, the effects of polymer and its coating onto fiber may be taken into consideration. Thus, the prepared PMF/CNFs green composites achieved here exhibit a stimuli-responsive mechanically dynamic nature, using water as the stimulus.

**Table 1.** Dynamic mechanical properties of dry and water swollen films of PMF/CNFs composites at 25 °C.

Composites	CNFs Content (% $v/v$ )	$E'$ at 25 °C (MPa)		
		Dry State	Wet State (After 4 Days of Swelling)	Wet State (After 6 Days of Swelling)
PMF/CNF-10	10	0.88	0.49	0.48
PMF/CNF-20	20	1.22	0.74	0.44
PMF/CNF-25	25	1.27	0.35	0.15

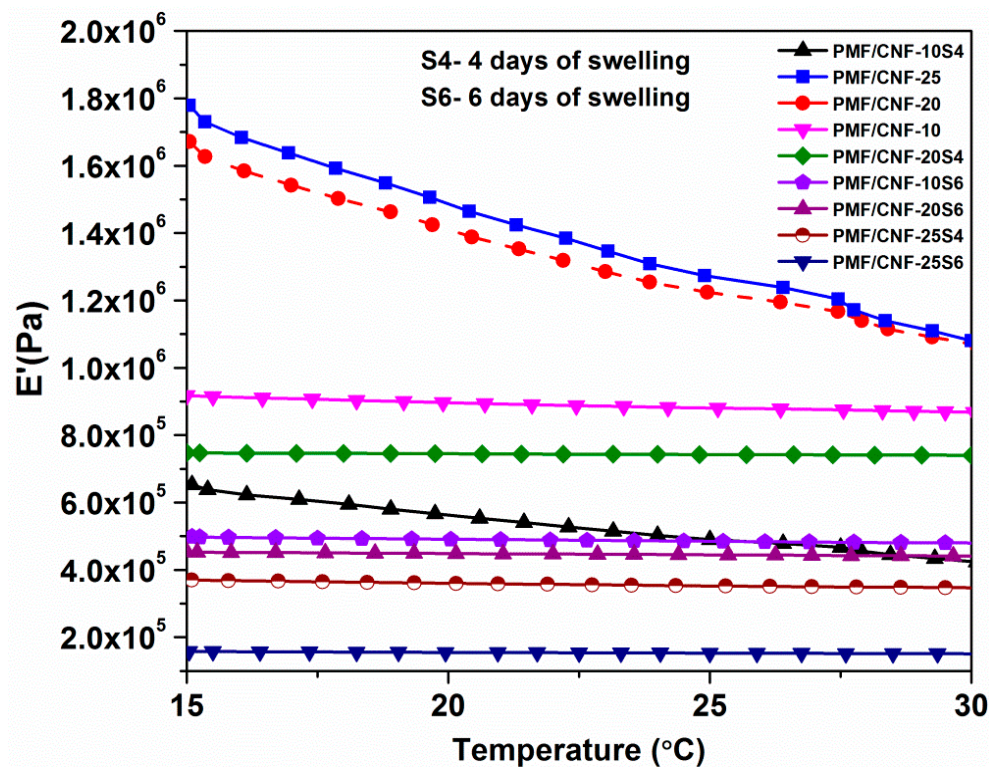


**Figure 7.** Tensile storage modulus ( $E'$ ) of dry and wet films of PMF/CNFs composites as a function of CNFs content.

It is to be noted that the dynamic behavior, i.e., measurement of storage modulus of composites, was calculated in tension mode. The pristine PMF elastomers are relatively low molecular weight polymers, and hence the preparation of good films was a challenge. With time, the films used to shrink and it was difficult to analyze the dynamic mechanical behavior in tension mode. With the introduction of cellulose filler in the PMF elastomer, the composite became stiff and non-shrinkable. So, the tensile storage modulus for the dry and the wet samples of the composite was analyzed.

#### 3.4. Force Modulation Technique in AFM for Imaging Biocomposites

It is an ideal technique for imaging composite materials to obtain contrast between regions of different stiffness i.e., soft and hard phases [28]. In this case, it was used to detect the change in mechanical properties (Modulus) of the composite surface in the dry and the swollen states. Figure 8 shows the topography and force modulation image of the dry and swollen sample (25% CNFs composite) obtained via contact mode in AFM imaging. Using the Hertzian contact mechanics or Hertzian model, for the dry PMF-20/CNFs composite the average modulus obtained was 82.7 MPa (taking 3 points). After swelling for 5 days, the wet composite showed a dramatic drop in the modulus to 32.3 MPa. This was due to the decrease in the local sample stiffness after swelling in water. This confirms the water sensitive nature of the prepared PMF/CNFs biobased composites via variations in the mechanical properties of the composite surface. Furthermore, the adhesion in the contact or adhesion energy values was obtained. Wet sample showed higher energy of adhesion compared to dry sample.

In FMM technique, a constant static load applied to the cantilever under compressive mode and the total force exerted on the surface of the sample is higher compared to the tension force applied via conventional dynamic analysis. Therefore, the modulus obtained from the AFM analysis is higher with respect to DMA measurement.



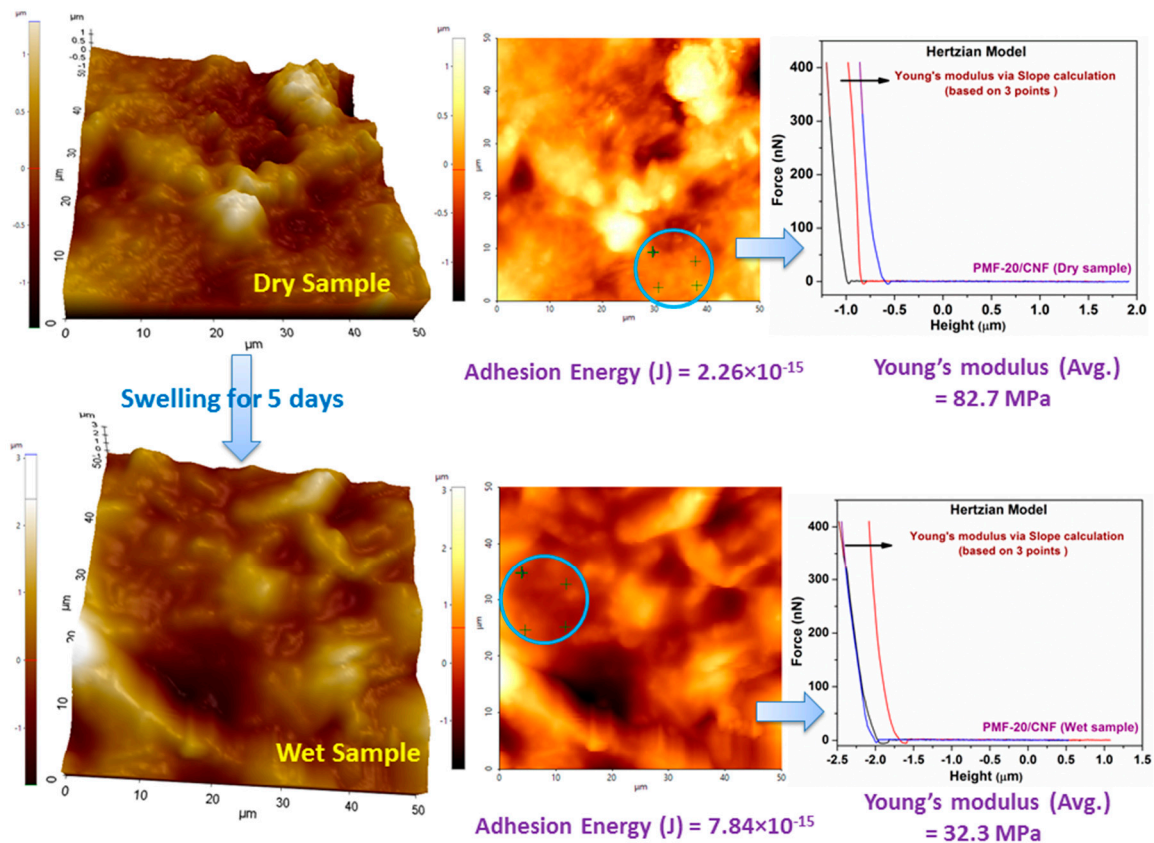


Figure 8. Topography and force modulation image of 25% CNF composite (dry and wet states).

### 3.5. Self-Healing Behavior of the PMF/CNF Composites

Due to the presence of a furan ring in the polymer matrix of the composite, the thermoreversible “DA Click reaction” was investigated for self-healing application. The presence of peaks at  $1015$  and  $1502$   $\text{cm}^{-1}$ , due to the breathing and stretching of the furan ring, are clearly shown in the FTIR spectra of the PMF/CNFs dry composites (Figure 9). On exposure to water, i.e., upon swelling, the furan peaks almost completely disappeared (Figure 9). So, the dry composite was used for the investigation of thermoreversible self-healing behavior instead of swollen samples. The composite containing 10% CNFs was used for all of the analysis in the self-healing study.

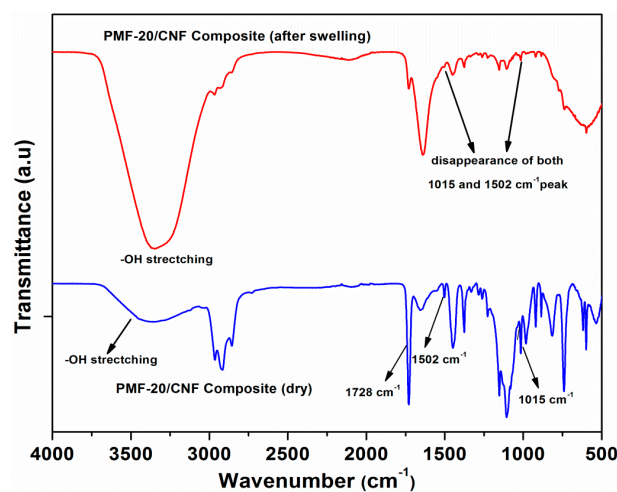


Figure 9. Fourier-transform infrared spectroscopy (FTIR) spectra of PMF-20/CNFs composite (before and after swelling in water).

It was clearly mentioned that the self-healing character of the biobased composite was investigated due to the presence of furan moiety in the pristine PMF polymer via the reversible Diels-Alder chemistry mechanism. Due to the presence of crosslinking between the bismaleimide and furan in PMF, the swelling percentage was observed as being much less (as mentioned earlier) for the composite. Upon swelling, the furan ring peak (FTIR spectra, Figure 9) in wet PMF/CNF composite disappeared. Therefore, the wet PMF/CNF composite does not respond to the self-healing test as followed for the dry composite.

The water-sensitive nature of the composites was also verified using force modulation microscopy (FMM) via AFM from the local stiffness value on a particular surface.

The thermoreversible behavior of the DA adduct was analyzed from the heating and cooling cycles of DSC thermogram. The temperature sweep experiment between  $-100$  and  $200$  °C at a scan rate of  $10$  °C/min was followed, as shown in Figure 10. The  $T_g$  of the pristine polymer (PMF-20) is observed at  $-35$  °C. From the second heating run of the PMF-20/CNF/BM adduct, a broad intense endothermic peak was observed around  $120$  to  $170$  °C, indicating the cleavage of DA cross linkages via the reverse reaction. The cooling curve exhibits a small hump and wide exothermic peak from  $\sim 60$  to  $100$  °C due to the regeneration of DA adducts. This is because the recovered furan and bismaleimide moieties reconnect again during the cooling process. This phenomenon proves that the PMF-20/CNF/BM adduct formed via the DA coupling reaction showed thermally amendable properties. This reaction was extensively studied for the pristine polymer and reported in our earlier communication [26].

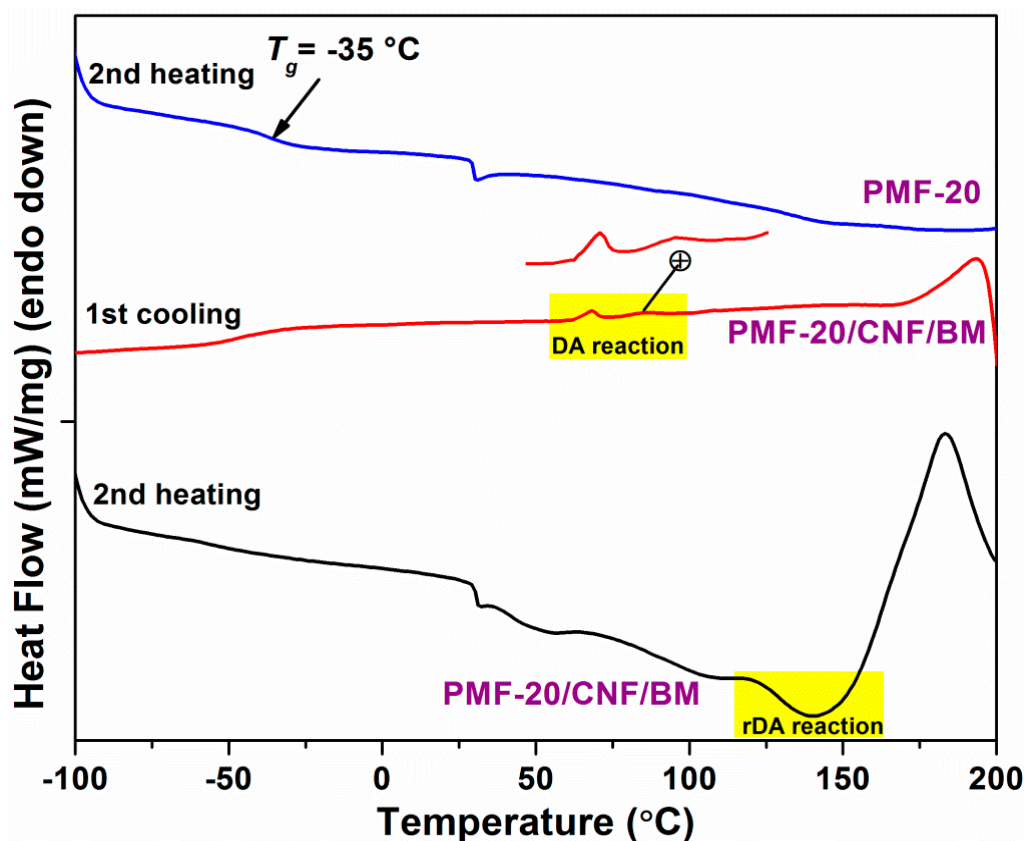
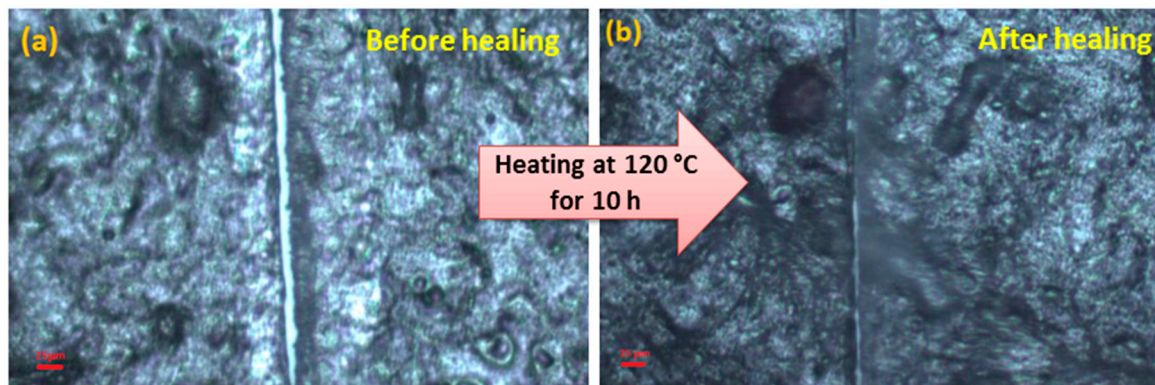


Figure 10. DSC plot of pristine PMF-20 and PMF/CNFs/BM DA-crosslinked adduct.

The self-healing character of the composites was monitored by optical microscopy. Initially, the images of the cut sample were observed (Figure 11a). The healing was performed by heating the cut samples at 120–130 °C for 10 h accompanied by subsequent cooling down to 60 °C and then to RT. The cut sample appeared to be almost healed for the composite/bismaleimide cross-linked films (Figure 11b), due to the possible DA reaction with the furan ring of the composite and bismaleimide. The circumstances follow the bond making and breaking process throughout the heating and cooling cycles.



**Figure 11.** Optical microscope images of (a) initial cut sample PMF/BM/CNFs films. (b) Healed images of PMF/BM/CNFs films after 10 h heating at 120 °C (Scale bar is 25 μm).

AFM analysis was also used to investigate the healing behavior of the cross-linked PMF-20/CNF/BM polymer. AFM is a wonderful and precise tool to produce damage on a polymer surface and to observe topographic changes for assessing the degree of healing. In our study, a surface scratch was made on the (PMF-20/CNF/BM) crosslinked film sample and the image was taken. Figure 12a,b represents the 3D height images of PMF-20/CNF/BM cross-linked polymer (before and after healing). The composite containing 10% CNFs has been used for the self-healing study, due to more rubbery nature of the material. After heating at 120 °C for 10 h, the depth of the cut area decreases dramatically. When the DA scratched film was heated at 120 °C for 10 h, the cyclo-adduct undergoes bond cleavage due to the reverse reaction, i.e., retro-DA reaction. On cooling down to 60 °C for a few hours and subsequently to room temperature, the breaking bonds reconnect again following the Diels-Alder reaction mechanism. Thus, the scratch was healed and the depth of the cut area decreased. For the calculation of healing efficiency, the depth of the cut was measured at two different positions from the 2D height images (Figure 12c,d) and an average was taken. The healing efficiency was obtained about 90%, verifying the thermoreversible self-healing behavior of the polymer composite using a crosslinker.

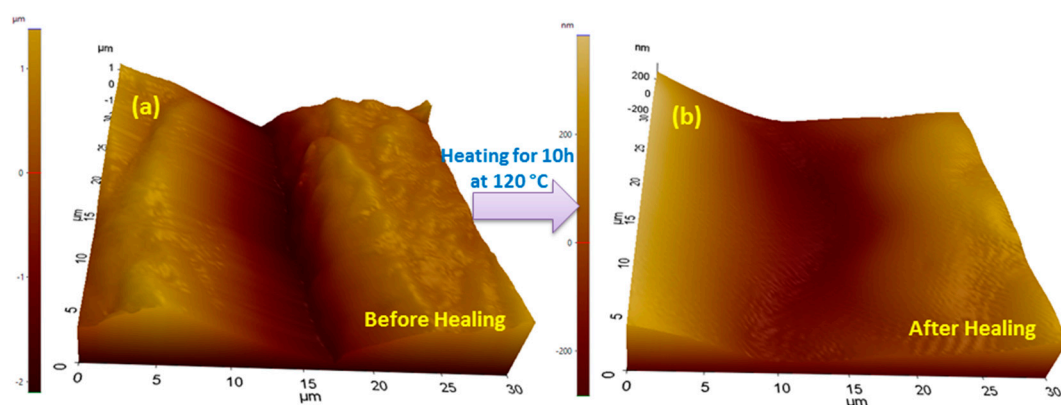


**Figure 12.** Cont.



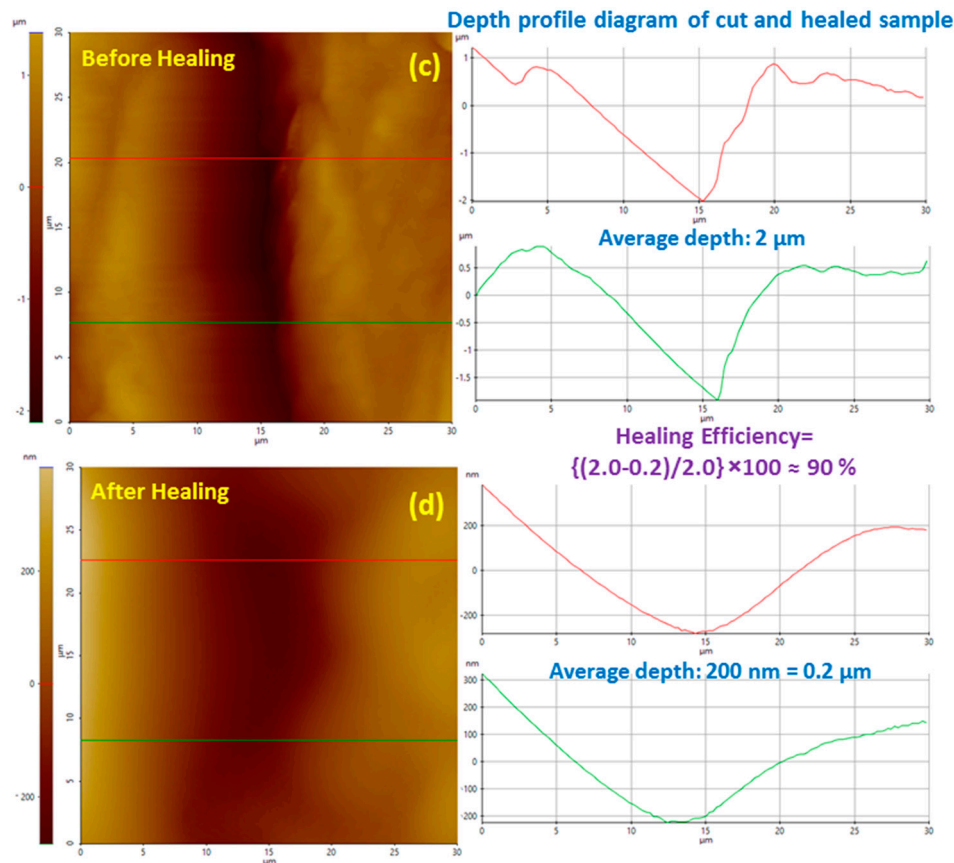


**Figure 12.** AFM images of cut sample (a) Height images of original cut and (b) healed sample at 120 °C for 10 h (c) 2D height images of original cut and (d) healed sample at 120 °C for 10 h.

#### 4. Conclusions

Cellulose-based green composites are currently regarded as one of the most promising areas of research and scientific development in the field of biobased products. Motivated by the desire to develop smart materials, biobased composites with stimuli-responsive behavior have been thought of. In this study, a green polymer composite was designed with the incorporation of hydrophilic cellulose nanofibrils into a biobased poly (MY-co-FMA) elastomer matrix. The composites exhibited stimuli-responsive character like mechanically adaptive behavior with water as the stimulus and a self-healing nature using bismaleimide as stimulus. The aqueous swelling character of composites was noticed to increase in a nonlinear manner with increasing nanofibril content, implying that the rate of water uptake is enhanced by the hydrophilic nature of cellulose. Furthermore, both the amount of water uptake and the modulus change of these composite depend strongly on the nanofibril content and the presence of the hydrophilic cellulose–cellulose and cellulose–polymer networks, which control the diffusion of water through the composite films. Upon exposure to water, hydrogen bonding between water molecules and surface hydroxyl groups of cellulose nanofibrils causes a notable reduction in the storage modulus ( $E'$ ) of the material. Water-responsive polymer composites prepared showed a modulus reduction from 1.27 (dry state) to 0.15 MPa (wet state) upon wetting/swelling. This type of observation suggests the potential use of these composite films in selective membranes for biomedical applications. The water sensitive nature of the composites using force modulation microscopy (FMM) via AFM showed the average modulus as 82.7 and 32.3 MPa for dry and swollen PMF-20/CNFs composite, respectively. The dry PMF/CNFs composite exhibited thermoreversible self-healing behavior following DA-click chemistry using crosslinker bismaleimide, examined by both optical microscopy and AFM analysis. The healing efficiency was obtained as about 90% from the AFM height images, confirming the thermoreversible nature of crosslinked DA-adduct at 120 °C

for 10 h. Thus, the composites prepared showed the dual-responsive properties of water sensitivity and self-healing using different external stimuli. This type of new-generation biobased elastomer composite could be valued as a class of sustainable smart materials and has great potential to replace petroleum-based products.

**Author Contributions:** Conceptualization, P.S. and A.K.B.; design of experiments, P.S.; writing-paper, P.S.; data analysis, P.S. and A.K.B.; review and editing, P.S., and A.K.B.; supervision, A.K.B.; All authors have read and agreed to the published version of the manuscript.

**Funding:** This research was funded by Council of Scientific and Industrial Research, HRDG, New Delhi, India (Ref. No: 20/12/2015(ii) EU-V).

**Acknowledgments:** The authors gratefully acknowledged IIT Kharagpur for all the support and necessary facilities. Pranabesh Sahu, pranabesh.cema@gmail.com, deeply thanks CSIR (HRDG), New Delhi, for providing financial support in terms of senior research fellowship (Ref. No: 20/12/2015(ii) EU-V).

**Conflicts of Interest:** The authors declare no conflict of interest.

## References

1. Hjerresen, D.L.; Schutt, D.L.; Boese, J.M. Green Chemistry and Education. *J. Chem. Educ.* **2000**, *77*, 1543–1547. [[CrossRef](#)]
2. Haack, J.A.; Hutchison, J.E. Green Chemistry Education: 25 Years of Progress and 25 Years Ahead. *ACS Sustain. Chem. Eng.* **2016**, *4*, 5889–5896. [[CrossRef](#)]
3. Llevot, A.; Dannecker, P.; Czapiewski, M.; Over, L.C.; Sçyler, Z.; Meier, M.A.R. Renewability is not enough: Recent advances in the sustainable synthesis of biomass-derived monomers and polymers. *Chem. Eur. J.* **2016**, *22*, 11510–11521. [[CrossRef](#)] [[PubMed](#)]
4. Zhu, Y.; Romain, C.; Williams, C.K. Sustainable polymers from renewable resources. *Nature* **2016**, *540*, 354–362. [[CrossRef](#)] [[PubMed](#)]
5. Lu, Y.; Larock, R.C. Novel polymeric materials from vegetable oils and vinyl monomers: Preparation, properties, and applications. *ChemSusChem* **2009**, *2*, 136–147. [[CrossRef](#)] [[PubMed](#)]
6. Williams, C.K.; Hillmyer, M.A. Polymers from renewable resources: A perspective for a special issue of polymer reviews. *Polym. Rev.* **2008**, *48*, 1–10. [[CrossRef](#)]
7. Silvestre, A.J.; Gandini, A. Terpenes: Major sources, properties and applications. In *Monomers Polymers and Composites from Renewable Resources*; Belgacem, M.N., Gandini, A., Eds.; Elsevier: Amsterdam, The Netherlands, 2008; pp. 17–38.
8. United States Department of Agriculture. USDA BioPreferred Program Guidelines How to Display and Promote the USDA Biobased Product Label, June 2016. Available online: <https://www.biopreferred.gov/BPResources/files/BioPreferredBrandGuide.pdf> (accessed on 23 June 2019).
9. Papageorgiou, G.Z. Thinking green: Sustainable polymers from renewable resources. *Polymers* **2018**, *10*, 952. [[CrossRef](#)]
10. Miller, S.A. Sustainable polymers: Opportunities for the next decade. *ACS Macro Lett.* **2013**, *2*, 550–554. [[CrossRef](#)]
11. Schneiderman, D.K.; Hillmyer, M.A. 50th anniversary perspective: There is a great future in sustainable polymers. *Macromolecules* **2017**, *50*, 3733–3749. [[CrossRef](#)]
12. Herbert, K.M.; Schrettl, S.; Rowan, S.J.; Weder, C. 50th anniversary perspective: Solid-State multistimuli, multiresponsive polymeric materials. *Macromolecules* **2017**, *50*, 8845–8870. [[CrossRef](#)]
13. Paul, D.R.; Robeson, L.M. Polymer nanotechnology: Nanocomposites. *Polymer* **2008**, *49*, 3187–3204. [[CrossRef](#)]
14. Qiao, R.; Brinson, L.C. Simulation of interphase percolation and gradients in polymer nanocomposites. *Compos. Sci. Technol.* **2009**, *69*, 491–499. [[CrossRef](#)]
15. La Mantia, F.P.; Morreale, M. Green composites: A brief review. *Compos. Part A* **2011**, *42*, 579–588. [[CrossRef](#)]
16. Mohanty, A.K.; Misra, M.; Drzal, L.T. Sustainable bio-composites from renewable resources: Opportunities and challenges in the green materials world. *J. Polym. Environ.* **2002**, *10*, 19–26. [[CrossRef](#)]
17. Behl, M.; Razzaq, M.Y.; Lendlein, A. Multifunctional shape-memory polymers. *Adv. Mater.* **2010**, *22*, 3388–3410. [[CrossRef](#)] [[PubMed](#)]
18. Gunes, I.S.; Jana, S.C. Shape memory polymers and their nanocomposites: A review of science and technology of new multifunctional materials. *J. Nanosci. Nanotechnol.* **2008**, *8*, 1616–1637. [[CrossRef](#)] [[PubMed](#)]

19. Abdul Khalil, H.P.S.; Bhat, A.H.; Ireana Yusra, A.F. Green composites from sustainable cellulose nanofibrils: A review. *Carbohydr. Polym.* **2012**, *87*, 963–979. [[CrossRef](#)]
20. Siqueira, G.; Bras, J.; Dufresne, A. Cellulosic bionanocomposites: A review of preparation, properties and applications. *Polymers* **2010**, *2*, 728–765. [[CrossRef](#)]
21. Dagnon, K.L.; Shanmuganathan, K.; Weder, C.; Rowan, S.J. Water-Triggered modulus changes of cellulose nanofiber nanocomposites with hydrophobic polymer matrices. *Macromolecules* **2012**, *45*, 4707–4715. [[CrossRef](#)]
22. Annamalai, P.K.; Dagnon, K.L.; Monemian, S.; Foster, E.J.; Rowan, S.J.; Weder, C. Water-Responsive mechanically adaptive nanocomposites based on styrene-butadiene rubber and cellulose nanocrystals—Processing matters. *ACS Appl. Mater. Interfaces* **2014**, *6*, 967–976. [[CrossRef](#)]
23. Mendez, J.; Annamalai, P.K.; Eichhorn, S.J.; Rusli, R.; Rowan, S.J.; Foster, E.J.; Weder, C. Bioinspired mechanically adaptive polymer nanocomposites with water-activated shape-memory effect. *Macromolecules* **2011**, *44*, 6827–6835. [[CrossRef](#)]
24. Montero De Espinosa, L.; Meesorn, W.; Moatsou, D.; Weder, C. Bioinspired polymer systems with stimuli-responsive mechanical properties. *Chem. Rev.* **2017**, *117*, 12851–12892. [[CrossRef](#)] [[PubMed](#)]
25. Tian, M.; Zhen, X.; Wang, Z.; Zou, H.; Zhang, L.; Ning, N. Bioderived rubber-cellulose nanocrystal composites with tunable water-responsive adaptive mechanical behavior. *ACS Appl. Mater. Interfaces* **2017**, *9*, 6482–6487. [[CrossRef](#)] [[PubMed](#)]
26. Sahu, P.; Bhowmick, A.K. Sustainable self-healing elastomers with thermoreversible network derived from biomass via emulsion polymerization. *J. Polym. Sci. Part A Polym. Chem.* **2019**, *57*, 738–751. [[CrossRef](#)]
27. Sahu, P.; Sarkar, P.; Bhowmick, A.K. Design of a molecular architecture via a green route for an improved silica reinforced nanocomposite using bioresources. *ACS Sustain. Chem. Eng.* **2018**, *6*, 6599–6611. [[CrossRef](#)]
28. Arnold, W. Force modulation in atomic force microscopy. In *Encyclopedia of Nanotechnology*; Bhushan, B., Ed.; Springer: Berlin/Heidelberg, Germany, 2012.



© 2020 by the authors. Licensee MDPI, Basel, Switzerland. This article is an open access article distributed under the terms and conditions of the Creative Commons Attribution (CC BY) license (<http://creativecommons.org/licenses/by/4.0/>).